

Dual-Task Mutual Learning for Semi-Supervised Medical Image Segmentation

Yichi Zhang¹ and Jicong Zhang^{1,2,3,4}

¹ School of Biological Science and Medical Engineering, Beihang University, Beijing, China

² Hefei Innovation Research Institute, Beihang University, Hefei, China

³ Beijing Advanced Innovation Centre for Biomedical Engineering, Beijing, China

⁴ Beijing Advanced Innovation Centre for Big Data-Based Precision Medicine, Beijing, China

Abstract. The success of deep learning methods in medical image segmentation tasks usually requires a large amount of labeled data. However, obtaining reliable annotations is expensive and time-consuming. Semi-supervised learning has attracted much attention in medical image segmentation by taking the advantage of unlabeled data which is much easier to acquire. In this paper, we propose a novel dual-task mutual learning framework for semi-supervised medical image segmentation. Our framework can be formulated as an integration of two individual segmentation networks based on two tasks: learning region-based shape constraint and learning boundary-based surface mismatch. Different from the one-way transfer between teacher and student networks, an ensemble of dual-task students can learn collaboratively and implicitly explore useful knowledge from each other during the training process. By jointly learning the segmentation probability maps and signed distance maps of targets, our framework can enforce the geometric shape constraint and learn more reliable information. Experimental results demonstrate that our method achieves performance gains by leveraging unlabeled data and outperforms the state-of-the-art semi-supervised segmentation methods⁵.

Keywords: Semi-supervised learning · Medical image segmentation · Mutual Learning · Signed distance maps.

1 Introduction

Medical image segmentation aims to understand images in pixel-level and label each pixel into a certain class, which is a fundamental step for many clinical applications [17, 19]. Recently, deep learning techniques have showed significant improvements and achieved state-of-the-art performances in many medical image segmentation tasks [2, 5, 10]. However, the success of deep neural networks usually relies on massive labeled dataset, while it is hard and expensive to obtain large-amount well-annotated data where only experts can provide reliable annotations

⁵ Our code will be available at <https://github.com/YichiZhang98/DTML>

for medical imaging. Unlabeled medical images are much easier to acquire and can be used in conjunction with labeled data to train segmentation models. As a result, semi-supervised learning has been widely explored to learn from a limited amount of labeled data and an arbitrary amount of unlabeled data [15], which is a fundamental, challenging problem and has a high impact on real-world clinical applications.

To utilize unlabeled data, a simple and intuitive method is to assign pseudo annotations to unlabeled data and then train the segmentation model using both labeled and pseudo labeled data. Pseudo annotations are commonly generated in an iterative approach wherein a model iteratively improves the quality of pseudo annotations by learning from its own predictions on unlabeled data [1]. Zhang *et al.* [25] introduced adversarial learning for biomedical image segmentation by encouraging the segmentation output of unlabeled data to be similar to annotations of labeled data. Although semi-supervised learning with pseudo annotations has shown promising performance, model-generated annotations can still be noisy and has detrimental effects to the subsequent segmentation model [12, 14].

Recent efforts in semi-supervised segmentation have been focused on incorporating unlabeled data into the training procedure with an unsupervised loss function. Some of these methods enforce the consistency between model predictions on the original data and the perturbed data by adding small perturbations to the unlabeled data. For example, Li *et al.* [7] proposed to constrain the consistency under transformation like rotation to utilize unlabeled data. Yu *et al.* [23] extended the mean teacher paradigm [18] with the guidance of uncertainty map for semi-supervised learning. Some other methods focus on enforcing the similar distribution of predictions using an adversarial loss [6, 14].

Signed distance maps (SDM) can provide an alternative to classical ground truth by transforming binary masks to gray-level images where the intensities of pixels are changed according to the distance to the closest boundary [9], which has been widely applied for medical image segmentation tasks to obtain further improvements by offering an implicit representation of the ground truth [4, 13]. Specifically, the network can be divided into two branches to generate the segmentation probabilistic maps and regress the signed distance maps at the same time. Due to the task difference, these two branches can learn different representations of segmentation targets from different perspectives, so as to obtain further improvements.

On the condition that the output of different tasks can be mapped to the same predefined space, instead of data-level regularization, we focus on building task-level regularization to utilize unlabeled data and propose a novel dual-task mutual learning framework for semi-supervised medical image segmentation. Our framework can be formulated as an integration of two individual segmentation networks based on the above two tasks: model M_s for generating the segmentation probabilistic maps and model M_d for regressing the signed distance maps. These two models share the same backbone network structure, and have task specific segmentation and regression heads. Following the mutual learning manner [24], different from the one-way transfer between teacher and student net-

works, we aim at encouraging dual-task networks to learn collaboratively and explore useful knowledge from each other during the training process. Under the semi-supervised learning setting, we only activate the supervised segmentation loss for labelled data, while cross-task consistency loss is activated for all training cases so as to utilize the unlabeled data. By jointly learning the segmentation probability maps and signed distance maps, our framework can enforce the geometric shape constraint and collaboratively learn more reliable information for segmentation throughout the training procedure.

Our method is evaluated on the Atrial Segmentation Challenge dataset for left atrium (LA) segmentation [21] with extensive comparisons to existing methods. The experimental results demonstrate that our method achieves performance gains by leveraging unlabeled data and outperforms the state-of-the-art semi-supervised segmentation methods.

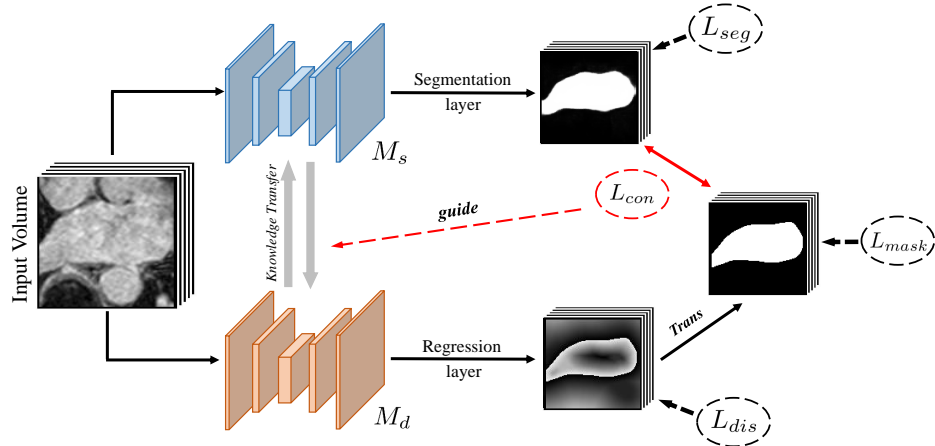


Fig. 1. The overview of our proposed dual-task mutual learning framework for semi-supervised medical image segmentation. The framework can be formulated as an integration of two individual segmentation networks, the upper one named M_s for generating the segmentation probabilistic maps and the lower one named M_d for regressing the signed distance maps. These two networks share the same backbone structure, and have task specific segmentation/regression output layers. During the training process, the networks are optimized with mutual learning manner to implicitly explore useful knowledge from each other.

2 Method

In this section, we introduce details about our proposed dual-task mutual learning framework. As illustrated in Figure 1, our framework can be formulated as an integration of two individual segmentation networks. These two networks share the same backbone structure and have specific segmentation and regression heads for different tasks. The upper one M_s aims at generating segmentation probabilistic maps while the lower one M_d aims at regressing the signed distance maps. Since the output of different tasks can be mapped to the same predefined space, dual-task networks can learn different representations of segmentation targets from different perspectives. We focus on building task-level regularization to enable each network learn from peer network’s guidance and introduce a cross-task consistency regularization to enforce the representation of predictions to be consistent. To fully utilize the spatial information, we task 3D volumes as the input for both networks.

2.1 Dual-Task Networks

Following the design of classic encoder-decoder architecture [3,11,16] to generate segmentation probabilistic maps, an auxiliary regression head is added to generate the signed distance maps composed by a 3D convolution block followed by the \tanh activation. The signed distance maps of ground truth G can be defined by

$$G_{SDF} = \begin{cases} - \inf_{y \in \partial G} \|x - y\|_2, & x \in G_{in} \\ 0, & x \in \partial G \\ + \inf_{y \in \partial G} \|x - y\|_2, & x \in G_{out} \end{cases} \quad (1)$$

where $\|x - y\|$ is the Euclidian distance between voxels x and y , and G_{in} , ∂G , G_{out} represents the inside, boundary and outside of the target object. In general, G_{SDF} takes negative values inside the target and positive values outside the object, and the absolute value is defined by the distance to the closest boundary point. To transform the output of signed distance maps to segmentation output, we utilize a smooth approximation to the inverse transform as in [8], which can be defined by

$$G_{mask} = \frac{1}{1 + e^{-k \cdot z}}, z \in G_{SDF} \quad (2)$$

where z is the value of signed distance maps at voxel x , and k is a transform factor selected as large as possible to approximate the transform. Our dual-task networks share the same backbone structure and differ at the end of the network. Specifically, for M_s only the segmentation head is activated, while for M_d only the regression head is activated. Given an input image $X \in R^{H \times W \times D}$, dual-task

networks M_s and M_d generate the confidence score map $\hat{Y}_{seg} \in [0, 1]^{H \times W \times D}$ and signed distance map $\hat{Y}_{dis} \in \mathbf{R}^{H \times W \times D}$ as follows

$$\hat{Y}_{seg} = f_{seg}(X; \theta_{seg}), \quad \hat{Y}_{dis} = f_{dis}(X; \theta_{dis}) \quad (3)$$

where θ_{seg} , θ_{dis} are corresponding parameters of segmentation network M_s and regression network M_d , respectively.

2.2 Mutual Learning for Semi-Supervised Segmentation

For semi-supervised segmentation of 3D medical images, where the training set contains M labeled cases and N unlabeled cases, we denote the labeled set as $D_L = \{X_i, Y_i\}_{i=1}^M$ and the unlabeled set as $D_U = \{Y_i\}_{i=1}^N$, where $X_i \in \mathbf{R}^{H \times W \times D}$ is the input volume and $Y_i \in \{0, 1\}^{H \times W \times D}$ is the corresponding ground truth. Since conventional supervised segmentation loss trains the network to approximate the annotations, to utilize unlabeled cases for training, instead of data-level regularization, we aim at building task-level regularization with our proposed dual-task mutual learning framework. Due to the task-level difference of networks, peer network can provide useful experience as the guidance for the training. To quantify the match of the two network's predictions, we focus on enforcing cross-task consistency between segmentation predictions and transformed regression predictions:

$$L_{con} = \|f_{seg}(X; \theta_{seg}) - f_{mask}^{-1}(f_{dis}(X; \theta_{dis}))\|^2 \quad (4)$$

where f_{mask}^{-1} is the transformation of signed distance maps to segmentation maps as described in (2).

For labeled cases, we employ the combination of dice loss and cross-entropy loss as the supervised loss \mathcal{L}_{seg} for the segmentation of M_s . While for M_d , supervision on output signed distance maps \mathcal{L}_{dis} and transformed segmentation maps \mathcal{L}_{mask} can both be employed for the training of M_d . However, we empirically found that supervised directly on segmentation maps with \mathcal{L}_{mask} can achieve better performance (See Sec. 3.2 for details). Therefore, the goal of our semi-supervised segmentation framework is to minimize the following combined functions

$$\min_{\theta_{seg}} \sum_{i=1}^N \mathcal{L}_{seg}(f_{seg}(X_i; \theta_{seg}), Y_i) + \sum_{i=1}^{N+M} \mathcal{L}_{con}(f_{mask}^{-1}(f_{dis}(X_i; \theta_{dis})), f_{seg}(X_i; \theta_{seg})) \quad (5)$$

$$\min_{\theta_{dis}} \sum_{i=1}^N \mathcal{L}_{mask}(f_{mask}^{-1}(f_{dis}(X_i; \theta_{dis})), Y_i) + \sum_{i=1}^{N+M} \mathcal{L}_{con}(f_{mask}^{-1}(f_{dis}(X_i; \theta_{dis})), f_{seg}(X_i; \theta_{seg})) \quad (6)$$

3 Experiments

3.1 Dataset and Implementation Details

We evaluate our method on the Left Atrium (LA) dataset from Atrial Segmentation Challenge ⁶ [21]. The dataset contains 100 3D gadolinium-enhanced MR imaging scans (GE-MRIs) and corresponding LA segmentation mask for training and validation. These scans have an isotropic resolution of $0.625 \times 0.625 \times 0.625 \text{ mm}^3$. Following the task setting in [23], we split the 100 scans into 80 scans for training and 20 scans for validation, and apply the same pre-processing methods. Out of the 80 training scans, we use the same 20%/16 scans as labeled data and the remaining 80%/64 scans as unlabeled data for semi-supervised segmentation task.

Our framework is implemented in PyTorch, using an NVIDIA Tesla V100 GPU. In this work, we use V-Net [11] as the backbone structure for all experiments to ensure a fair comparison. To incorporate signed distance maps for mutual learning, an auxiliary regression head is added at the end of the original V-Net. We use the Stochastic Gradient Descent (SGD) optimizer to update the network parameters for 6000 iterations, with an initial learning rate (lr) 0.01 decayed by 0.1 every 2500 iterations. The batch size is 4, consisting of 2 labeled images and 2 unlabeled images. We randomly crop $112 \times 112 \times 80$ sub-volumes as the network input and the final segmentation results are obtained using a sliding window strategy. We use the standard data augmentation techniques on-the-fly to avoid overfitting during the training procedure [22], including randomly flipping, and rotating with 90, 180 and 270 degrees along the axial plane.

We use four complementary evaluation metrics to quantitatively evaluate the segmentation results. Dice similarity coefficient (Dice) and Jaccard Index (Jaccard), two region-based metrics, are used to measure the region mismatch. Average surface distance (ASD) and 95% Hausdorff Distance (95HD), two boundary-based metrics, are used to evaluate the boundary errors between the segmentation results and the ground truth.

3.2 Ablation Analysis

We conduct detailed experimental studies to examine the effectiveness of our proposed framework. For supervised loss of M_d , L_2 loss between the output signed distance maps and transformed distance maps of ground truth named \mathcal{L}_{dis} , and segmentation loss between transformed segmentation mask of output SDM and binary ground truth mask named \mathcal{L}_{mask} can both be employed for the training. We make an comparison between different settings for M_d . It can be observed from Table 1 that using \mathcal{L}_{mask} for supervised loss can obtain higher performance compared with using \mathcal{L}_{dis} or their sum. Experimental results demonstrate that direct supervision based on segmentation masks for both M_s and M_d is the best practice for our framework since minor differences on signed distance maps

⁶ <http://atriaseg2018.cardiacatlas.org/data/>

Table 1. Comparison of different supervised loss functions for our dual-task mutual learning framework. All the models follow the same task setting with 16 labeled scans and 64 unlabeled scans for training.

Supervised Loss M_s/M_d	Metrics			
	Dice[%]	Jaccard[%]	ASD[voxel]	95HD[voxel]
DTML($\mathcal{L}_{seg}/\mathcal{L}_{dis}$)	89.72	81.55	1.97	7.64
DTML($\mathcal{L}_{seg}/\mathcal{L}_{mask}$)	90.12	82.14	1.82	7.01
DTML($\mathcal{L}_{seg}/\mathcal{L}_{dis} + \mathcal{L}_{mask}$)	89.89	81.82	1.93	6.61

Table 2. Ablation analysis of our dual-task mutual learning framework.

Method	Scans used		Metrics			
	Labeled	Unlabeled	Dice[%]	Jaccard[%]	ASD[voxel]	95HD[voxel]
M_s only	16	0	86.03	76.06	3.51	14.26
M_d only	16	0	88.69	79.91	3.12	11.62
DTML	16	0	89.17	80.68	2.13	7.82

may somehow mislead the training. Besides, to analyze the effectiveness of our method, we conduct experiments to implement our method with only labeled cases and remove the cross-task consistency loss between dual-task networks for comparison. The first and second rows in Table 2 are segmentation results of M_s and M_d training independently. We can observe that our method significantly outperforms both tasks training independently on all metrics. Paired T-test shows that the improvements are statistically significant at $p < 0.05$, validating the effectiveness of our mutual learning framework. In Figure 2, we show some segmentation examples of supervised method and our proposed semi-supervised method for visual comparison. We can observe that our segmentation results have higher overlap ratio with the ground truth.

3.3 Comparison with Other Semi-supervised Methods

To demonstrate the effectiveness of our method, a comprehensive comparison with existing methods is conducted. We evaluate our method in with comparisons to state-of-the-art semi-supervised segmentation methods, including ASDNet [14], TCSE [7], UA-MT [23], DTC [8], SASS [6] and Double-Uncertainty [20]. To ensure a fair comparison, we used the same V-Net backbone in these methods. The results of comparison experiments are shown in Table 3. As can be observed, our method achieves better performance on all the evaluation metrics compared with state-of-the-art methods. Besides, our method can leverage unlabeled data without requiring any iterative update schemes, which reduces the computational cost and running time.

Table 3. Quantitative comparison between our methods and other semi-supervised methods. All the models use the same V-Net as the backbone. The first and second rows are upper-bound performance and fully supervised baseline. Experimental results demonstrate that our method outperforms the state-of-the-art results consistently.

Method	Scans used		Metrics			
	Labeled	Unlabeled	Dice[%]	Jaccard[%]	ASD[voxel]	95HD[voxel]
V-Net	80	0	91.14	83.82	1.52	5.75
V-Net	16	0	86.03	76.06	3.51	14.26
ASDNet [14]	16	64	87.90	78.85	2.08	9.24
TCSE [7]	16	64	88.15	79.20	2.44	9.57
UA-MT [23]	16	64	88.88	80.21	2.26	7.32
DTC [8]	16	64	89.42	80.89	2.10	7.32
SASS [6]	16	64	89.54	81.24	2.20	8.24
DoubleUnc [20]	16	64	89.65	81.35	2.03	7.04
DTML (Ours)	16	64	90.12	82.14	1.82	7.01

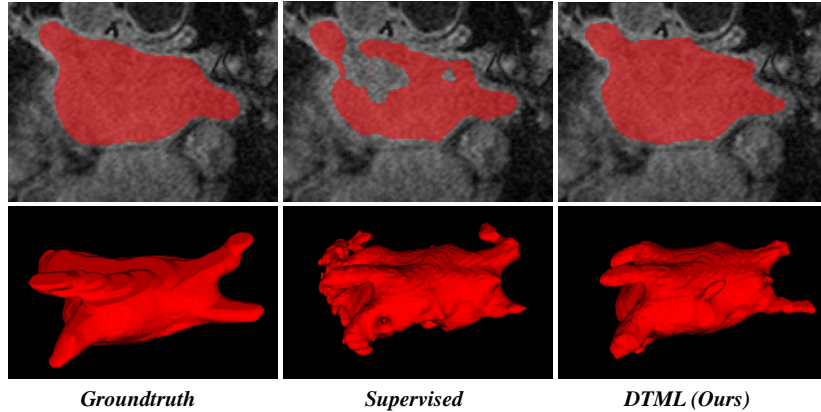


Fig. 2. Examples of 2D and 3D visual comparison of different segmentation results.

4 Conclusion

In this paper, we propose a novel dual-task mutual learning framework for semi-supervised medical image segmentation. Our method can effectively leverage abundant unlabeled data by encouraging the output consistency of two tasks: learning region-based shape constraint and learning boundary-based surface mismatch. By jointly learning the semantic segmentation and signed distance maps of targets and building task-level regularization, our framework can enforce the geometric shape constraint and collaboratively learn more reliable information from unlabeled images throughout the training procedure. Comprehensive experimental analysis demonstrates the effectiveness of our proposed method and

significant improvement compared with state-of-the-art semi-supervised segmentation methods.

Acknowledgment

This work is supported by the National Key Research and Development Program of China (2016YFF0201002), the University Synergy Innovation Program of Anhui Province (GXXT-2019-044), and the National Natural Science Foundation of China (61301005).

References

1. Bai, W., Oktay, O., Sinclair, M., Suzuki, H., Rajchl, M., Tarroni, G., Glocker, B., King, A., Matthews, P.M., Rueckert, D.: Semi-supervised learning for network-based cardiac mr image segmentation. In: International Conference on Medical Image Computing and Computer-Assisted Intervention. pp. 253–260. Springer (2017)
2. Bernard, O., Lalande, A., Zotti, C., Cervenansky, F., Yang, X., Heng, P.A., Cetin, I., Lekadir, K., Camara, O., Ballester, M.A.G., et al.: Deep learning techniques for automatic mri cardiac multi-structures segmentation and diagnosis: is the problem solved? *IEEE Transactions on Medical Imaging* **37**(11), 2514–2525 (2018)
3. Çiçek, Ö., Abdulkadir, A., Lienkamp, S.S., Brox, T., Ronneberger, O.: 3d u-net: learning dense volumetric segmentation from sparse annotation. In: International conference on medical image computing and computer-assisted intervention. pp. 424–432. Springer (2016)
4. Dangi, S., Linte, C.A., Yaniv, Z.: A distance map regularized cnn for cardiac cine mr image segmentation. *Medical physics* **46**(12), 5637–5651 (2019)
5. Heller, N., Isensee, F., Maier-Hein, K.H., Hou, X., Xie, C., Li, F., Nan, Y., Mu, G., Lin, Z., Han, M., et al.: The state of the art in kidney and kidney tumor segmentation in contrast-enhanced ct imaging: Results of the kits19 challenge. *Medical Image Analysis* p. 101821 (2020)
6. Li, S., Zhang, C., He, X.: Shape-aware semi-supervised 3d semantic segmentation for medical images. In: International Conference on Medical Image Computing and Computer-Assisted Intervention. pp. 552–561. Springer (2020)
7. Li, X., Yu, L., Chen, H., Fu, C.W., Xing, L., Heng, P.A.: Transformation-consistent self-ensembling model for semisupervised medical image segmentation. *IEEE Transactions on Neural Networks and Learning Systems* (2020)
8. Luo, X., Chen, J., Song, T., Chen, Y., Wang, G., Zhang, S.: Semi-supervised medical image segmentation through dual-task consistency. *arXiv preprint arXiv:2009.04448* (2020)
9. Ma, J., Wei, Z., Zhang, Y., Wang, Y., Lv, R., Zhu, C., Gaoxiang, C., Liu, J., Peng, C., Wang, L., et al.: How distance transform maps boost segmentation cnns: an empirical study. In: *Medical Imaging with Deep Learning*. pp. 479–492. PMLR (2020)
10. Ma, J., Zhang, Y., Gu, S., Zhang, Y., Zhu, C., Wang, Q., Liu, X., An, X., Ge, C., Cao, S., et al.: Abdomenct-1k: Is abdominal organ segmentation a solved problem? *arXiv preprint arXiv:2010.14808* (2020)
11. Milletari, F., Navab, N., Ahmadi, S.A.: V-net: Fully convolutional neural networks for volumetric medical image segmentation. In: 2016 fourth international conference on 3D vision (3DV). pp. 565–571. IEEE (2016)

12. Min, S., Chen, X., Zha, Z.J., Wu, F., Zhang, Y.: A two-stream mutual attention network for semi-supervised biomedical segmentation with noisy labels. In: Proceedings of the AAAI Conference on Artificial Intelligence. vol. 33, pp. 4578–4585 (2019)
13. Navarro, F., Shit, S., Ezhov, I., Paetzold, J., Gafita, A., Peek, J.C., Combs, S.E., Menze, B.H.: Shape-aware complementary-task learning for multi-organ segmentation. In: International Workshop on Machine Learning in Medical Imaging. pp. 620–627. Springer (2019)
14. Nie, D., Gao, Y., Wang, L., Shen, D.: Asdnet: attention based semi-supervised deep networks for medical image segmentation. In: International conference on medical image computing and computer-assisted intervention. pp. 370–378. Springer (2018)
15. Qi, G.J., Luo, J.: Small data challenges in big data era: A survey of recent progress on unsupervised and semi-supervised methods. *IEEE Transactions on Pattern Analysis and Machine Intelligence* (2020)
16. Ronneberger, O., Fischer, P., Brox, T.: U-net: Convolutional networks for biomedical image segmentation. In: International Conference on Medical image computing and computer-assisted intervention. pp. 234–241. Springer (2015)
17. Sykes, J.: Reflections on the current status of commercial automated segmentation systems in clinical practice. *Journal of Medical Radiation Sciences* **61**(3), 131 (2014)
18. Tarvainen, A., Valpola, H.: Mean teachers are better role models: Weight-averaged consistency targets improve semi-supervised deep learning results. In: Proceedings of the 31st International Conference on Neural Information Processing Systems. pp. 1195–1204 (2017)
19. Van Ginneken, B., Schaefer-Prokop, C.M., Prokop, M.: Computer-aided diagnosis: how to move from the laboratory to the clinic. *Radiology* **261**(3), 719–732 (2011)
20. Wang, Y., Zhang, Y., Tian, J., Zhong, C., Shi, Z., Zhang, Y., He, Z.: Double-uncertainty weighted method for semi-supervised learning. In: International Conference on Medical Image Computing and Computer-Assisted Intervention. pp. 542–551. Springer (2020)
21. Xiong, Z., Xia, Q., Hu, Z., Huang, N., Bian, C., Zheng, Y., Vesal, S., Ravikumar, N., Maier, A., Yang, X., et al.: A global benchmark of algorithms for segmenting the left atrium from late gadolinium-enhanced cardiac magnetic resonance imaging. *Medical Image Analysis* **67**, 101832 (2021)
22. Yu, L., Cheng, J.Z., Dou, Q., Yang, X., Chen, H., Qin, J., Heng, P.A.: Automatic 3d cardiovascular mr segmentation with densely-connected volumetric convnets. In: International conference on medical image computing and computer-assisted intervention. pp. 287–295. Springer (2017)
23. Yu, L., Wang, S., Li, X., Fu, C.W., Heng, P.A.: Uncertainty-aware self-ensembling model for semi-supervised 3d left atrium segmentation. In: International Conference on Medical Image Computing and Computer-Assisted Intervention. pp. 605–613. Springer (2019)
24. Zhang, Y., Xiang, T., Hospedales, T.M., Lu, H.: Deep mutual learning. In: Proceedings of the IEEE Conference on Computer Vision and Pattern Recognition. pp. 4320–4328 (2018)
25. Zhang, Y., Yang, L., Chen, J., Fredericksen, M., Hughes, D.P., Chen, D.Z.: Deep adversarial networks for biomedical image segmentation utilizing unannotated images. In: International Conference on Medical Image Computing and Computer-Assisted Intervention. pp. 408–416. Springer (2017)